Lignin Peroxidase Oxidation of Veratryl Alcohol: Effects of the Mutants H82A, Q222A, W171A, and F267L[†]

Maarten D. Sollewijn Gelpke,[‡] Jooyoung Lee,[§] and Michael H. Gold*

Department of Biochemistry and Molecular Biology, OGI School of Science & Engineering, Beaverton, Oregon 97006-8921

Received October 15, 2001; Revised Manuscript Received January 2, 2002

ABSTRACT: The site-directed mutations H82A and Q222A (residues near the heme access channel), and W171A and F267L (residues near the surface of the protein) were introduced into the gene encoding lignin peroxidase (LiP) isozyme H8 from *Phanerochaete chrysosporium*. The variant enzymes were produced by homologous expression in *P. chrysosporium*, purified to homogeneity, and characterized by kinetic and spectroscopic methods. The molecular masses, the p*I*s, and the UV−vis absorption spectra of the ferric and oxidized states of these LiP variant enzymes were similar to those of wild-type LiP (wtLiP), suggesting the overall protein and heme environments were not significantly affected by these mutations. The steady-state and transient-state parameters for the oxidation of veratryl alcohol (VA) by the H82A and Q222A variants were very similar to those of wtLiP, demonstrating that these residues are not involved in VA oxidation and that the heme access channel is an unlikely site for VA oxidation. In contrast, the W171A variant was unable to oxidize VA, confirming the apparent essentiality of Trp171 in VA oxidation by LiP. The kinetic rates of spontaneous LiP compound I reduction in the absence of VA were similar for W171A and wild-type LiP, suggesting that there may not be a radical formed on the Trp171 residue of LiP in the absence of VA. For the F267L variant, both the $K_{m\ app}$ value in the steady state and the apparent dissociation constant (K_D) for compound II reduction were greater than those for wtLiP. These results indicate that the site including W171 and F267, rather than the heme access channel, is the site of VA binding and oxidation in LiP. Whereas Trp171 appears to be essential for VA oxidation, it apparently is not independently responsible for the spontaneous decomposition of oxidized intermediates. The nearby Phe267 apparently is also involved in VA binding.

The lignin-degrading basidiomycete *Phanerochaete chrysosporium* secretes two families of class II extracellular peroxidases: lignin peroxidase (LiP)[1] and manganese peroxidase (MnP) (*1*, *2*). These enzymes, along with an H_2O_2-generating system, are the major components of the extracellular lignin-degrading system in this fungus (*1*, *3*−*5*). Lignin peroxidase isozyme H8 (LiPH8) from *P. chrysosporium* catalyzes the H_2O_2-dependent oxidation of nonphenolic lignin model compounds via formation of a substrate aryl cation radical, with subsequent nonenzymatic reactions yielding the final oxidized products (*6*−*9*). Veratryl alcohol (VA), a secondary metabolite secreted by *P. chrysosporium* and a LiP substrate, stimulates the LiP-catalyzed oxidations of synthetic lignin (*10*), proteins (*11*, *12*), and a variety of lignin model compounds and aromatic pollutants (*13*−*16*).

LiPH8 is a monomeric heme protein with a molecular mass of 42 kDa and a p*I* of 3.3 (*1*, *4*, *17*). Early spectroscopic studies indicated that the heme iron of native LiPH8 is ferric, high-spin, and pentacoordinate, with a histidyl fifth ligand (*18*−*21*). Analyses of the LiPH8 crystal structure (*22*, *23*) and amino acid sequence comparisons with other heme peroxidases (*1*, *24*) demonstrate that important catalytic residues, including the proximal His176, the H-bonded Asp238, and the distal His47, Arg43, Phe46, and Asn84 residues, are all conserved within the heme pocket. These results indicate that the heme environment of LiP is similar to that of MnP and other fungal and plant peroxidases (*1*, *2*).

Spectroscopic and kinetic studies of the LiP native enzyme and its oxidized intermediates demonstrate that the catalytic cycle of LiP is also similar to that of MnP, horseradish peroxidase (HRP), and other plant and fungal peroxidases (*25*−*28*). Native LiP undergoes a two-electron oxidation by H_2O_2, yielding compound I (LiPI) (*25*, *26*). The one-electron reduction of LiPI by reducing substrates, such as veratryl alcohol (VA), yields compound II (LiPII) and a VA cation radical ($VA^{+\bullet}$). A second one-electron reduction returns the

[†] This research was supported by Grant DE-FG03-96ER20235 from the Division of Energy Biosciences, U.S. Department of Energy (to M.H.G.).

* To whom correspondence should be addressed at the Department of Biochemistry and Molecular Biology, OGI School of Science & Engineering, 20000 N.W. Walker Rd., Beaverton, OR 97006-892l. Telephone: 503-748-1076; Fax: 503-748-1464; E-mail: mhgold@myexcel.com.

[‡] Present address: Joint Genome Institute, U.S. Department of Energy, 2800 Mitchell Dr., Walnut Creek, CA 94598.

[§] Present address: Department of Genetics, Virginia Polytechnic Institute and State University, Blacksburg, VA 24060.

[1] Abbreviations: ABTS, 2,2′-azinobis(3-ethylbenzothiazoline-6-sulfonate); DFAD, 4-[(3,5-difluoro-4-hydroxyphenyl)azo]benzenesulfonic acid; *gpd*, glyceraldehyde-3-phosphate dehydrogenase; HCHN, high-carbon, high-nitrogen; HRP, horseradish peroxidase; IEF, isoelectric focusing; LiP, lignin peroxidase; LiPI, -II, -III, and -III*, LiP compounds I, II, III, and III*; LiPH8, LiP isozyme H8; MnP, manganese peroxidase; rLiP, recombinant LiP; SDS−PAGE, sodium dodecyl sulfate−polyacrylamide gel electrophoresis; VA, veratryl alcohol (3,4-dimethoxy benzyl alcohol);$VA^{+\bullet}$, VA cation radical; wtLiP, wild-type LiP.

10.1021/bi011930d CCC: $22.00
Published on Web 02/02/2002

enzyme to the ferric oxidation state, completing the catalytic cycle (*25, 26, 29*). In the absence of a reducing substrate, excess H_2O_2 converts native LiP to LiP compound III* (LiPIII*), an inactive form of the enzyme (*30, 31*). VA can convert LiPIII* back to the native enzyme, thus rescuing the inactive enzyme (*31*).

Recent detailed crystal structure analyses and structure−function studies of LiP indicate that Trp171 may be part of the VA interaction site of LiP. Mutation of the Trp171 residue, which is hydroxylated at the Cβ in wtLiP (*32*), suggests Trp171 is involved in VA oxidation (*33*). An electron-transfer pathway from Trp171 to the heme was proposed (*32, 33*); however, the mechanism of this oxidation reaction remains unclear.

Previously, we developed a homologous expression system for LiPH8 (*34*) in which the *P. chrysosporium* glyceraldehyde-3-phosphate dehydrogenase (*gpd*) gene promoter is used to drive the expression of the *lipH8* gene during primary metabolic growth when endogenous LiP and MnP are not expressed (*34*). In the present study, four site-directed mutants of LiPH8 (H82A, Q222A, W171A, and F267L) were produced using our homologous expression system. The variant enzymes were used to investigate the site of VA oxidation and the role of VA in the LiP catalytic cycle.

MATERIALS AND METHODS

Organisms. *P. chrysosporium* wild-type strain OGC101 (*35*), auxotrophic strain OGC316-7 (Ura11) (*36*), and prototrophic transformants where maintained as described previously (*37*). *Escherichia coli* DH5α was used for subcloning plasmids.

Construction of Expression Plasmids. Site-directed mutations were introduced in the *lipH8* gene (*24*) component of the LiPH8 homologous expression vector, pUGL (*34*), using the Quikchange (Stratagene) protocol. pUGL contains 1.1 kb of the *P. chrysosporium gpd* gene promoter fused to the *P. chrysosporium lipH8* gene at their respective TATA box sites (*34*). The pUGL plasmid also contains the *Schizophyllum commune ura1* gene (*38*) as a selectable marker (*34*). Forward and reverse primers were designed to construct four expression plasmids containing the H82A, W171A, Q222A, or F267L mutations. The complete *lipH8* coding region, including the mutation sites, of each mutated expression plasmid was verified by double-stranded sequencing.

Transformation of the Uracil Auxotroph Ura11. Protoplasts of *P. chrysosporium* Ura11 were transformed with *Eco*RI-linearized mutant pUGL plasmids as described previously (*36, 39*). Prototrophic transformants were transferred to minimal medium slants, and conidia from these slants were used to inoculate liquid stationary cultures as described previously (*34, 40*). After 3 days of growth at 28 °C, the extracellular medium was assayed for either LiP activity or protein, either using the 2,2′-azinobis(3-ethylbenzothiazoline-6-sulfonate) (ABTS) assay (*41*) with 0.5 mM ABTS and 0.1 mM H_2O_2 or by western blotting using a polyclonal LiP antibody (*24*). Positive transformant clones, producing recombinant mutant LiP enzyme, were purified by isolating single basidiospores as described previously (*35*), followed by final selection of the transformant strains.

Enzyme Production and Purification. The selected transformants were grown for 2 days at 37 °C from conidial inocula as stationary cultures in 1-L flasks, containing 80 mL of high-carbon, high-nitrogen (HCHN) medium, containing 2% glucose and 12 mM NH_4 tartrate, supplemented with 0.2% tryptone (*34*). Homogenized mycelial mats from the stationary cultures were used as inocula for 1-L HCHN cultures in 2-L flasks, supplemented with 3 mM VA and 0.1% Tween 80. The 1-L cultures were incubated at 28 °C for 4 days at 150 rpm on a rotary shaker (*34*). The extracellular medium of 14 1-L HCHN cultures was harvested and subjected to successive steps of hollow-fiber ultrafiltration (10 kDa cutoff, Amicon), Phenyl-Sepharose chromatography, Sephadex G-100 size exclusion chromatography, and FPLC-MonoQ anion exchange column chromatography as described previously (*34, 40*). Wild-type LiPH8 was produced and isolated as described previously (*31, 42*).

SDS−PAGE and Isoelectric Focusing. SDS−PAGE was performed using a 10% Tris−glycine gel system and a Miniprotean II apparatus (BioRad); the BioRad SDS−PAGE Low Range marker mix was used. Isoelectric focusing (IEF) electrophoresis was performed using the Pharmacia Phast-system with IEF Phastgels (pH 3−9), and the Sigma IEF Mix 3.6−6.6 marker kit. All gels were stained with Coomassie blue.

Enzyme Assays and Spectroscopic Procedures. Electronic absorption spectra of the various oxidation states of the LiP enzymes and steady-state kinetic data were collected at room temperature, using a Shimadzu UV-260 spectrophotometer. The wild-type or mutant LiP compound I oxidized state was prepared by mixing equimolar amounts of enzyme and H_2O_2 in water. The LiP compound II oxidized state was prepared by mixing equimolar amounts of enzyme and ferrocyanide in water followed by 1 equiv of H_2O_2. Enzyme concentrations were determined at 407 nm using an extinction coefficient of 133 mM^{-1} cm^{-1} (*42*). H_2O_2 concentrations were determined using $\epsilon_{240} = 43.6$ M^{-1} cm^{-1} (*43*).

VA and ABTS oxidation pH profiles by the wild-type and mutant enzymes were obtained by measuring the specific activity of the oxidation reactions conducted in 20 mM sodium succinate buffer at pH values from 3.0 to 6.0. For the oxidation of VA to veratrylaldehyde, the reaction mixture (1 mL) contained 2 μg of LiP, 2 mM VA, and 0.1 mM H_2O_2 in sodium succinate (20 mM); veratraldehyde formation was followed at 310 nm ($\epsilon_{310} = 9.3$ M^{-1} cm^{-1}). The ABTS oxidation reactions (1 mL) contained 0.5 mM ABTS, 0.1 mM H_2O_2, and 2 μg of LiP, and were followed at 405 nm ($\epsilon_{405} = 36.6$ M^{-1} cm^{-1}) (*33, 41*).

Steady-state kinetic analysis for the oxidation of VA and ferrocyanide yielded apparent K_m and k_{cat} values which were calculated from linear double-reciprocal plots of the rates of oxidation versus varying substrate concentrations. VA oxidation was measured at 310 nm, and the initial rates were determined in the presence of 2 μg of enzyme/mL in 20 mM sodium succinate (pH 3.0). The oxidation of ferrocyanide to ferricyanide was measured at 420 nm [$\epsilon_{420} = 1$ mM^{-1} cm^{-1} (*44*)], using various concentrations of ferrocyanide in the presence of 0.2 mM H_2O_2 and 2 mg/mL LiP.

Transient-State Kinetics. Transient-state kinetic measurements were conducted at 25 ± 0.1 °C using an Applied Photophysics stopped-flow reaction analyzer (SX.18MV) with sequential mixing and a diode array detector for rapid scanning spectroscopy. LiPI formation was measured at 397

nm, an isosbestic point between compounds I and II, by mixing 2 μM native enzyme in 20 mM sodium succinate (pH 3.0) with a 10−50-fold molar excess of H_2O_2 in the same buffer. LiPI reduction was measured at 417 nm in reaction mixtures containing 2 μM compound I and at least a 10-fold molar excess of VA in 20 mM sodium succinate (pH 3.0 or 4.5). LiPI was first prepared by premixing equimolar amounts of enzyme and H_2O_2 in H_2O, and its formation was confirmed by diode array scanning. The reduction of LiPII was measured at 407 nm in reaction mixtures containing 2 μM LiPII and at least a 10-fold molar excess of VA in 20 mM sodium succinate (pH 3.0). LiPII was prepared by mixing equimolar amounts of enzyme and ferrocyanide in water, followed by 1 equiv of H_2O_2 in water; formation of LiPII was confirmed by diode array scanning. Typically, six substrate concentrations were used in triplicate measurements. Curve-fitting was performed using the manufacturer's software.

UV−Vis Spectroscopic Analysis of Reactions of wtLiP and W171A. Stopped-flow diode array spectra were obtained for reactions of native wtLiP and W171A with excess H_2O_2, using a reaction mixture of ~4 μM enzyme and a 65-fold molar excess of H_2O_2 in 20 mM sodium succinate (pH 4.0). Absorption spectra were collected over 15.4 s. The stability of LiPI was investigated by incubation of ~2 μM compound I in 20 mM sodium succinate at pH 3.0, 4.0, 4.5, and 6.0. Compound I was first prepared by premixing equimolar amounts of enzyme and H_2O_2 in water. The spontaneous decay of compound I was followed at 417 nm.

Reactions of wtLiP and W171A with VA were also assessed using stopped-flow diode array scanning. Compound I was prepared as described above, using ~2 μM enzyme, and was incubated with a 10^3-fold molar excess of VA in 20 mM sodium succinate (pH 4.5). Absorption spectra were collected over 8 s. Absorption spectra were also collected for reactions of the W171A variant enzyme under steady-state conditions. Native W171A enzyme (4 μM) was incubated with 65-fold molar excess of H_2O_2 in 20 mM sodium succinate (pH 4.5), followed by the addition of 10^3-fold molar excess of VA, or the enzyme was incubated with 10^3-fold molar excess of VA in 20 mM sodium succinate (pH 4.5), followed by addition of 65-fold molar excess of H_2O_2.

Chemicals. Hydrogen peroxide 30% (w/w) solution was obtained from Sigma. VA was obtained from Aldrich and was purified by vacuum distillation. All other chemicals were reagent grade. Solutions were made in HPLC-grade water obtained from Aldrich.

RESULTS

Expression and Purification of the Mutant Enzymes. The *P. chrysosporium* homologous expression system for LiP (*34*) was used to express the variant LiP enzymes H82A, Q222A, W171A, and F267L in the extracellular medium of HCHN-agitated cultures. The expression constructs for each of the variant enzymes were used to transform the uracil auxotrophic strain Ura11 (OGC316-7), resulting in the isolation of at least 20 transformants for each mutation. Twelve transformants of each mutation were grown in HCHN stationary cultures and screened for extracellular LiP activity using the ABTS assay or by identifying extracellular LiP enzyme using western blots. Selected transformants, which produced LiP enzyme in sufficient quantities, were further purified by isolating single basidiospores (*35*), and after rescreening, one isolate for each mutation was selected to obtain the strains H82A-T2:4, Q222A-T3:1, W171A-T6:1, and F267L-T8:1. Each of these transformant strains expressed extracellular recombinant LiP (rLiP) when grown in HCHN shake cultures at 28 °C for 4 days, conditions under which endogenous peroxidases are not expressed (*34*, *40*). The variant LiPs were purified to homogeneity as determined by SDS−PAGE and IEF. The molecular masses of the LiP variants (~42 kDa) and the p*I* values (~3.3) were similar to those of wtLiP (Figure 1). The yields of expressed variant enzymes were 0.5−1.5 mg/L, which is comparable to that of recombinant wild-type LiPH8 (*34*). Typically, mutant enzymes were purified to R_z values of >3.

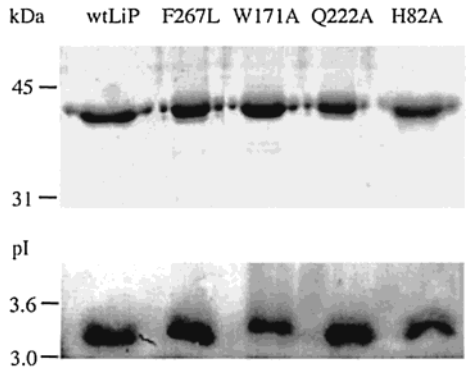

FIGURE 1: Molecular mass and p*I* determination of wtLiP and the LiP variants F267L, W171A, Q222A, and H82A LiP. (A) SDS−PAGE using a 10% Tris−glycine gel and (B) IEF using a Phastgel 3−9 of wild-type and LiP variants, showing similar M_r and p*I* for each enzyme.

Spectral Properties of the LiP Mutant Enzymes. The electronic absorption spectra of the native enzyme and oxidized intermediates, compounds I and II, for each of the LiP variant enzymes were essentially identical to those of the wild-type enzyme, as shown in Figure 2 for wtLiP and W171A, suggesting that substitutions of Ala for H82, Q222, and W171, and Leu for F267, do not significantly alter the heme environment of the protein.

Steady-State Kinetics. To assess the oxidation of VA by the wild-type and variant LiPs under steady-state conditions, linear double-reciprocal plots of initial oxidation rates were obtained over a range of H_2O_2 and VA concentrations. The apparent k_{cat} values for VA oxidation and the apparent K_m and k_{cat}/K_m values for VA and H_2O_2 are listed in Table 1. The apparent k_{cat} values for the H82A, Q222A, and F267L variants decreased only ~1.2-fold compared to that of wtLiP. In contrast, the W171A variant enzyme lost all VA oxidation activity. The apparent K_m values were similar between the H82A, Q222A, and wtLiP enzymes. However, the F267L variant exhibited a 3-fold increase in the apparent K_m, suggesting that this residue may also be involved in the oxidation of VA by LiP. The $k_{cat\ app}$, $K_{m\ app}$, and k_{cat}/K_m values for ferrocyanide oxidation by wtLiP and variant LiPs were essentially identical for wtLiP and all LiP variants (Table 2).

pH Profiles for the Oxidation of VA and ABTS. The specific activity for the oxidation of VA and ABTS was measured over a range of pH values for wtLiP and the LiP

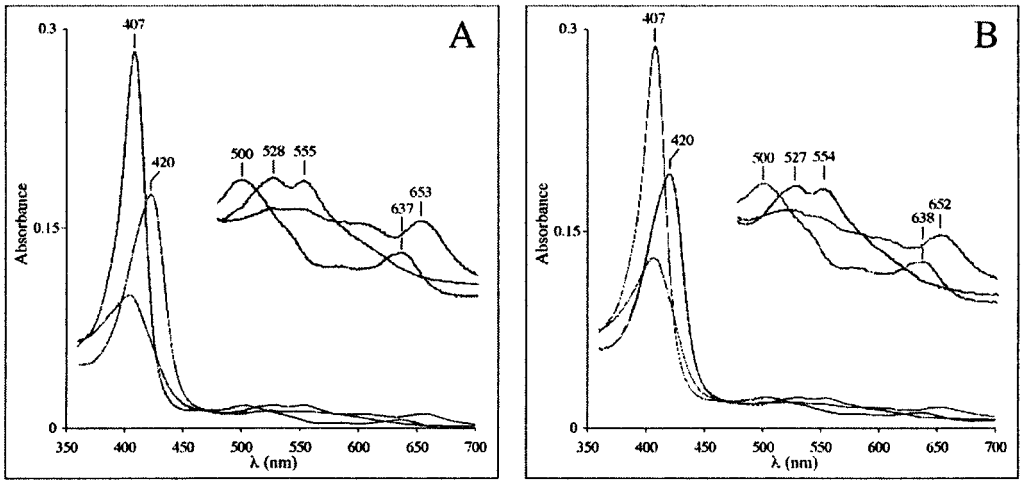

FIGURE 2: Electronic absorption spectra of the native enzyme and oxidized intermediates, compounds I and II, are shown for wtLiP (A) and for the W171A variant enzyme (B). Samples contained ~2 μM enzyme, and the intermediates were produced as described in the text.

Table 1: Kinetic Parameters for the Steady-State Oxidation of VA by wtLiP and LiP Mutants[a]

		VA		H_2O_2	
enzyme	k_{cat} (s^{-1})	K_m (μM)	k_{cat}/K_m ($M^{-1}\,s^{-1}$)	K_m (mM)	k_{cat}/K_m ($M^{-1}\,s^{-1}$)
wtLiP	19.9	102.9	2.5×10^5	48.6	4.8×10^5
W171A	na[b]	nr[c]	nr	nr	nr
Q222A	15.6	92.8	1.9×10^5	39.6	4.4×10^5
H82A	15.9	111.7	1.7×10^5	53.1	3.2×10^5
F267L[c]	15.1	295.1	0.5×10^5	50.7	3.0×10^5

[a] Reactions were carried out in 20 mM potassium succinate, pH 3.0. Apparent K_m and k_{cat} values for VA were determined using 0.1 mM H_2O_2, and apparent K_m and k_{cat} values for H_2O_2 were determined using 0.4 mM VA. [b] na = no detectable activity. [c] nr = no reaction.

Table 2: Steady-State Kinetic Parameters for the Oxidation of Ferrocyanide by Wild-Type and Variant LiP Enzymes[a]

enzyme	k_{cat} (s^{-1})	K_m (μM)	k_{cat}/K_m ($M^{-1}\,s^{-1}$)
wtLiP	65.8	48.5	1.4×10^6
W171A	60.8	65.4	0.9×10^6
Q222A	53.2	71.8	0.7×10^6
H82A	76.4	64.0	1.2×10^6
F267L	61.5	57.1	1.1×10^6

[a] Reactions were carried out in 20 mM potassium succinate (pH 3.0). Apparent K_m and k_{cat} values for ferrocyanide oxidation were determined using 0.2 mM H_2O_2.

variant enzymes (Figure 3). The specific activity for VA oxidation by wtLiP was highest at pH 3.0 and decreased gradually to <1 s^{-1} near pH 6.0. The H82A, Q222A, and F267L variants exhibited a similar decrease in specific activities over the pH range of 3.0−6.0, while the W171A variant did not oxidize VA over this entire pH range. The specific activities for ABTS oxidation also exhibited a gradual decrease with increasing pH, varying from ~30−50 s^{-1} at pH 3.0 to <2 s^{-1} at pH 5.5, for wtLiP as well as the LiP mutants (Figure 3).

Transient-State Kinetics. Transient-state kinetic rate constants were determined for each step in the LiP catalytic cycle. The kinetic traces for LiPI formation exhibited exponential character from which observed pseudo-first-order rate constants (k_{1obs}) were calculated. The k_{1obs} values were linearly proportional to H_2O_2 concentrations at 10−50-fold excess (data not shown). The apparent second-order rate

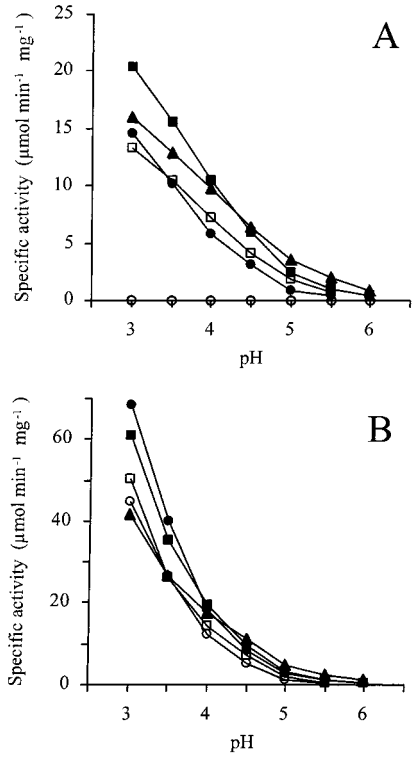

FIGURE 3: pH profiles for the specific activities of VA (panel A) and ABTS (panel B) oxidation by the wild-type (■), H82A (●), Q222A (▲), F267L (□), and W171A (○) LiP variants. The oxidation reactions were performed in 20 mM sodium succinate buffer, using 2 μg of enzyme, 0.1 mM H_2O_2, and 2 mM VA or 0.5 mM ABTS.

constants (k_{1app}) for LiPI formation were similar for the wild-type and mutant LiP enzymes (Table 3).

At pH 3.0 and 4.5, exponential kinetic traces were obtained for wtLiP, H82A, Q222A, and F267L compound I reduction, yielding observed pseudo-first-order rate constants (k_{2obs}) over a range of VA concentrations. The obtained k_{2obs} values were linearly proportional to the VA concentration for these enzymes, resulting in apparent second-order rate constants (k_{2app}) for LiPI reduction (Table 3). The k_{2app} values at pH 3.0 were very similar for H82A, Q222A, and wtLiP; however, the k_{2app} value for F267L was decreased by ~2-fold. At pH 4.5, the k_{2app} values for H82A, Q222A, F267L,

Table 3: Kinetic Parameters for the Formation of LiP Compound I by H_2O_2 and Reduction of Compound I by VA in Wild-Type and Variant LiP Enzymes[a]

	compound I formation	compound I reduction by VA	
		k_{2app} (M^{-1} s^{-1})	
enzyme	k_{1app} (M^{-1} s^{-1})	pH 3.0	pH 4.5
wtLiP	$(4.67 \pm 0.04) \times 10^5$	$(9.70 \pm 0.08) \times 10^5$	$(5.82 \pm 0.08) \times 10^5$
Q222A	$(4.58 \pm 0.08) \times 10^5$	$(8.82 \pm 0.11) \times 10^5$	$(4.12 \pm 0.07) \times 10^5$
H82A	$(4.39 \pm 0.06) \times 10^5$	$(8.70 \pm 0.07) \times 10^5$	$(5.71 \pm 0.04) \times 10^5$
F267L	$(4.42 \pm 0.04) \times 10^5$	$(4.20 \pm 0.07) \times 10^5$	$(3.75 \pm 0.05) \times 10^5$
W171A	$(4.83 \pm 0.06) \times 10^5$	nc[b]	nc

[a] Reactions were performed in 20 mM potassium succinate (pH 3.0 or 4.5) as indicated, using ~1 μM enzyme. The formation of compound I was monitored as the decrease of the native enzyme peak at 397 nm. The reduction of compound I in the presence of VA was monitored at 417 nm. [b] nc = not calculated.

Table 4: Kinetic Parameters for LiP Compound II Reduction by VA in Wild-Type and Variant LiP Enzymes[a]

	compound II reduction by VA		
enzyme	k_3 (s^{-1})	K_D (μM)	k_{3app} (M^{-1} s^{-1})
wtLiP	34.0 ± 0.2	$(1.82 \pm 0.05) \times 10^2$	1.85×10^5
Q222A	32.8 ± 0.5	$(1.80 \pm 0.08) \times 10^2$	1.82×10^5
H82A	26.4 ± 0.4	$(1.60 \pm 0.07) \times 10^2$	1.65×10^5
F267L	41.1 ± 0.5	$(6.58 \pm 0.13) \times 10^2$	0.63×10^5
W171A	na[b]	nr[c]	nr

[a] Reactions were performed in 20 mM potassium succinate (pH 3.0) using ~2 μM enzyme and were monitored at 407 nm. [b] na = no detectable activity. [c] nr = no reaction.

and wtLiP were similar but were slightly decreased compared to those at pH 3.0. The kinetic traces for W171A compound I reduction in the presence of VA also exhibited exponential character at various pHs, but the rates were in the range of the spontaneous rate of reduction. The k_{app} value was very low, suggesting that compound I reduction does not correlate with VA oxidation. The k_{2obs} values were low and stayed in the range of the k_{2obs} value of the spontaneous decay of W171A LiPI to LiPII.

For LiP compound II reduction by VA, exponential kinetic traces were obtained for wtLiP and the H82A, Q222A, and F267L variants, yielding observed pseudo-first-order rate constants (k_{3obs}) for VA concentrations of 25 μM to 2 mM. The plots of k_{3obs} values versus the VA concentration were hyperbolic, indicating saturation kinetics (*29*). The first-order rate constants (k_3) and the dissociation constants (K_D) were calculated from the least-squares fit of k_{3obs} values versus the VA concentration, and are shown in Table 4. The k_3 values for H82A, Q222A, F267L, and wtLiP were similar. However, the K_D for the F267L variant increased ~4-fold compared to the K_D of H82A, Q222A, and wtLiP. No W171A compound II reduction by VA was detected.

Spectroscopic Analysis of W171A. The reactions of both the wtLiP and W171A native enzyme with H_2O_2 were investigated. Stopped-flow diode array spectra of the enzymes in the presence of excess H_2O_2 clearly show the conversion of native enzyme to compound I and subsequent conversion to compound III*, evidenced by the shift in the Soret peak to 419 nm and the appearance of peaks at 545 and 578 nm in the visible region (Figure 4). Addition of excess VA to wild-type LiPIII* results in the conversion of compound III* to native enzyme, followed by the catalytic turnover of VA oxidation, as shown previously (*31*). In contrast, addition of excess VA to W171A compound III* did not result in its conversion to native enzyme or compound II. Instead, a slow decrease in absorbance intensity with no shift in the peaks occurred (data not shown).

The stability of compound I in wtLiP and the W171A variant was assessed in 20 mM sodium succinate at pH 3.0, 4.0, 4.5, and 6.0. The single-wavelength traces (417 nm) of the spontaneous reduction of compound I were exponentials from which observed rate constants (k_{obs}) were calculated (Table 5). The k_{obs} values of spontaneous compound I reduction were similar for wtLiP and W171A at each assessed pH level.

Under steady-state VA oxidation conditions, the W171A variant formed compound III*. Native W171A enzyme was incubated with excess VA, followed by the addition of excess H_2O_2. Absorption spectra were collected from 3 ms to 32.4 s after the start of the reaction as a series of 15 spectra distributed logarithmically (Figure 5). The native W171A enzyme was rapidly oxidized to compound I by H_2O_2, which was followed by a slow conversion of compound I to compound II, and subsequent conversion of compound II to compound III*. The oxidized intermediates were identified by absorption maxima in the 480−700 nm range (Figure 5).

Spectroscopic Analysis of Reactions with VA. Electronic absorption spectra of the W171A and wtLiP native enzymes and oxidized intermediates, compounds I and II, were essentially identical (Figure 2). Diode array absorption spectra of the incubation of W171A compound I with excess VA in buffer showed that W171A compound I is converted to compound II over ~8 s (Figure 5A). In contrast, transient-state kinetic analysis shows that wild-type LiPI is reduced rapidly to native enzyme in the presence of excess VA, with a k_{2app} value for compound I reduction of 5.82×10^5 M^{-1} s^{-1} and a k_{3app} value for LiPII reduction of $\sim 5.5 \times 10^4$ M^{-1} s^{-1} (*29*) under these conditions. Incubation of W171A compound II, prepared with equimolar amounts of ferrocyanide and H_2O_2, with excess VA did not alter the absorption spectrum (data not shown).

DISCUSSION

Lignin peroxidase catalyzes the one-electron oxidation of nonphenolic lignin model compounds with high redox potentials via the formation of a substrate aryl cation radical (*3, 4, 6*−*8, 46*). However, the detailed mechanism by which LiP degrades polymeric lignin remains unclear. *P. chrysosporium* and other LiP-producing fungi secrete VA (*4, 47*), which has been found to stimulate the depolymerization of synthetic lignin and the oxidation of a variety of recalcitrant substrates by LiP (*12, 48*−*50*). Several mechanisms have been proposed to account for the stimulation of LiP reactions by VA. Studies suggest that VA acts as a redox mediator in the oxidation of lignin and some model substrates (*12, 16, 48, 51*). Other studies suggest that VA aids the enzyme in completing its catalytic cycle during the oxidation of at least some substrates (*49, 52*).

Previously, we developed a homologous expression system to produce active *P. chrysosporium* LiPH8 (*34*). This system was used to produce variant LiPs altered in residues, which may be involved in the oxidation of VA and other substrates. The W171A mutant enzyme was used to reexamine a recently proposed site for VA oxidation (*33*). The F267L

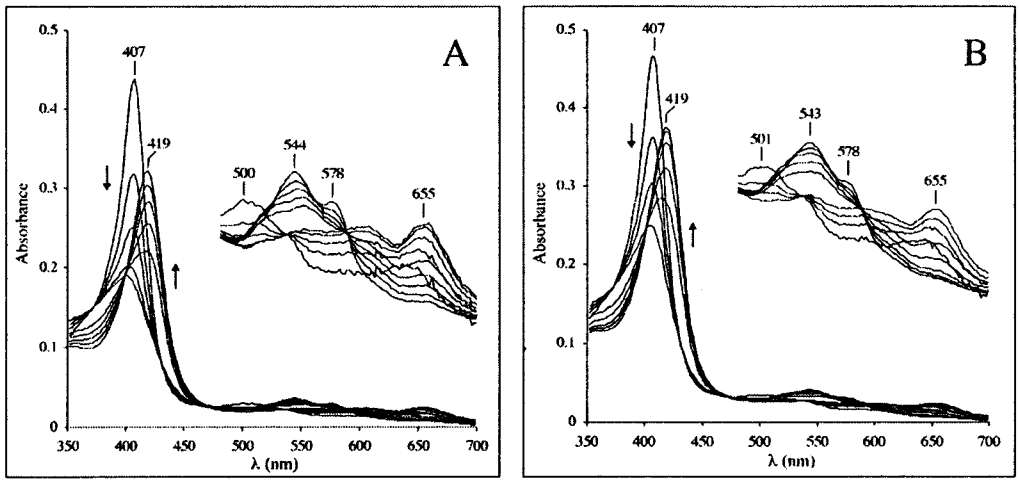

FIGURE 4: Reaction of the wtLiP and W171A variant with H_2O_2. Stopped-flow spectra of the wtLiP (A) and the W171A variant (B) incubated with 65-fold molar excess of H_2O_2 in 20 mM sodium succinate (pH4.0), using ~4 μM of each enzyme. The arrows indicate decrease or increase of absorption values over time. The series of spectra were collected at logarithmic intervals between 3 ms and 15.4 s, starting with 5 spectra from 3 to 40 ms, followed by 5 spectra from 1.1 to 15.4 s (A), or starting with 4 spectra from 3 to 27 ms, followed by 5 spectra from 1.1 to 15.4 s (B).

Table 5: Observed Rates for Spontaneous Reduction of Compound I in the Wild-Type and W171A Variant[a]

	k_{obs} (s^{-1})	
pH	wtLiP	W171A
3.0	6.5 ± 0.4	6.0 ± 0.3
4.0	2.2 ± 0.3	2.9 ± 0.3
4.5	$(8.0 \pm 0.4) \times 10^{-1}$	$(9.6 \pm 0.5) \times 10^{-1}$
6.0	$(5.0 \pm 0.5) \times 10^{-2}$	$(2.0 \pm 0.1) \times 10^{-2}$

[a] Equimolar amounts of enzyme and H_2O_2 were premixed to form compound I in 20 mM sodium succinate at the indicated pH.

mutant was used to assess the role of this residue, which is in proximity to Trp171. The H82A and Q222A mutant enzymes were used to investigate the role of the heme access channel, another proposed site for VA oxidation (*23, 53*) and possibly an alternative substrate oxidation site. The recombinant variant enzymes all have molecular masses, p*I*s, and absorption spectra similar to wtLiP, suggesting that the variant proteins are produced and secreted without significant changes in either their overall structures or their heme environments.

Crystal structure data show that amino acids H82 and Q222 are located in the heme access channel of LiP (*22, 23*), which is the apparent site of substrate oxidation for other peroxidases such as HRP, *Coprinus* peroxidase, and ascorbate peroxidase (*54*). A binding mode for VA involving H82 and Q222 was previously proposed, based on modeling studies (*23, 53*). A third amino acid residue at the heme access channel, E146, was mutated in previous studies, resulting in a ~2−3-fold reduced VA oxidation activity (*33, 55*) and a significant increase in the pK_a for the oxidation of the small, negatively charged dye 4-[(3,5-difluoro-4-hydroxyphenyl)-azo]benzenesulfonic acid (DFAD) (*33*). The decrease in VA oxidation activity for these variants was minor compared to the large effect of the W171F and W171S mutations on VA oxidation (*33*). E146 does appear to control the low-pH optimum for the oxidation of DFAD, suggesting that the heme access channel may be the productive site for this particular substrate (*33*). However, E146 is conserved in both MnP and LiP enzymes, suggesting a function that is not specific for LiP.

Since both His82 and Q222 were originally proposed to be part of the VA binding site (*23, 53*), we decided to examine the effects of mutations of these two residues on the oxidation of VA, ferrocyanide, and ABTS. Steady-state kinetic analyses of VA oxidation by LiP show that the apparent K_m values for these variants are similar to that of wtLiP, whereas the apparent k_{cat} values for these mutants are only slightly reduced compared to wtLiP. In addition, the pH profiles of VA oxidation were similar for H82A, Q222A, and wtLiP enzymes. These results suggest that the H82A and Q222A mutations have little effect on VA oxidation and, therefore, are unlikely to be components of the VA binding site in LiP. Since Glu146 is also in the heme access channel, our results suggest that this residue is unlikely to affect VA oxidation directly. Thus, the decrease in VA oxidation in the E146G mutant reported earlier (*33*) is probably due to an indirect effect such as a small change in enzyme structure or in an important salt bridge.

Transient-state kinetic analyses of the individual steps in the LiP catalytic cycle also show that the H82A and Q222A mutations do not have a significant effect on the formation of LiPI by H_2O_2 or the reduction of the oxidized intermediates, LiPI and LiPII, by VA. Thus, residues His82 and Gln222, which are located at the heme access channel, do not affect the binding or oxidation of VA, suggesting that the heme access channel is an unlikely VA binding site in LiP. Analysis of the steady-state oxidation of ferrocyanide showed essentially identical k_{cat} and K_m values for wtLiP and the H82A and Q222A variant proteins. Furthermore, the pH profiles for the oxidation of ABTS by wtLiP and H82A and Q222A mutants were similar. Together, these results suggest that residues His82 and Gln222 are not involved in the oxidation of ABTS, ferrocyanide, or VA. This strongly suggests that VA does not bind at the heme access channel.

Our results confirm that Trp171 is essential for VA oxidation (*33*). Incubation of the W171A variant enzyme with excess VA and H_2O_2 results only in the formation of inactive compound III* with no measurable oxidation of VA, suggesting that Trp171 is essential for VA oxidation. Transient-state kinetic studies indicate that VA was able to reduce W171A compound I to compound II at essentially

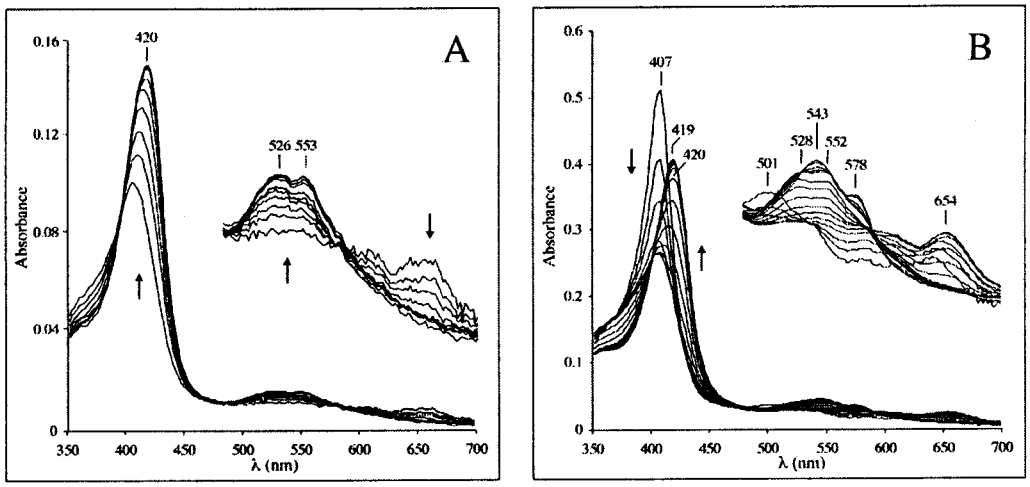

FIGURE 5: Reactions of the W171A variant LiP with VA and H_2O_2. (A) Stopped-flow spectra of W171A compound I reduction by VA, using ~4 μM enzyme and 1000-fold molar excess of VA, in 20 mM sodium succinate (pH 4.5). Spectra were collected from 9 ms to 8 s with logarithmic intervals. (B) Stopped-flow spectra of the steady-state oxidation of VA by W171A in the presence of ~4 μM enzyme, a 65-fold molar excess of H_2O_2, and a 1000-fold molar excess of VA, in 20 mM sodium succinate (pH 4.5). A series of 15 spectra was collected from 3 ms to 32.4 s, distributed logarithmically. The arrows indicate a decrease or increase of absorption values at the wavelength indicated over time.

the spontaneous rate of decay of this intermediate (Tables 3 and 5). The dependence of this rate on VA was very small or nonexistent. VA was unable to reduce W171A compound II.

Spectroscopic studies confirm that VA cannot reduce compound I to compound II at any significant rate. The full reduction of compound I took 8 s. Finally, VA was unable to reduce W171A compound II to native enzyme. Incubation of W171A compound II with excess VA showed no change in the absorption spectrum at pH 4.5. At lower pH, only spontaneous decay of compound II to native enzyme occurred. In addition, VA was unable to protect the W171A mutant enzyme from inactivation, nor did it convert the inactivated W171A compound III* back to native enzyme as has been shown for wtLiP (*31*). Absorption spectra collected during incubation of the enzyme under steady-state conditions (Figure 5) clearly demonstrate the conversion of native enzyme to compound III*. Thus, it appears that VA is unable to reduce the oxidized states of the W171 variant to the native enzyme, confirming an essential role for Trp171 in the catalytic mechanism.

The instability of both W171A and wtLiP compound I and the rates of spontaneous decay (*26*, *27*) were assessed to investigate the role of Trp171 in electron transfer. Previously, a so-called "rapid phase" in the spontaneous decay of wtLiP compound I, that was not present in the W171F variant enzyme, was assigned to the transfer of an electron from Trp171 to the heme (*33*). However, these rates were determined by incubating native enzyme with excess H_2O_2 rather than with equimolar amounts (*33*).

Our results show that the incubation of native W171A or wild-type enzyme with excess H_2O_2 results in the rapid formation of compound I, followed by its conversion to compound III*, as clearly shown by the absorption peaks at 543 and 578 nm (Figure 4). The latter conversion results from several reactions, including the decay of compound I to compound II, followed by conversion of compound II to compound III and compound III to compound III* by H_2O_2 (*30*, *31*). In addition, the so-called rapid phase for compound I conversion was observed by Doyle et al. in a single-wavelength trace at 412 nm (*33*), although the isosbestic point between LiP compounds I and II is located around 417 nm (*29*), thereby further complicating the analysis of their kinetic traces. Moreover, the proposed rate for a spontaneous electron transfer of ~2.3 s^{-1} (*33*) is much too slow to support the VA oxidation k_{cat} of around 20 s^{-1}.

Incubation of LiP compound I, prepared by mixing equimolar amounts of enzyme and H_2O_2, resulted in spontaneous decay for both wtLiP and W171A at several pH levels. The decay of compound I was exponential over time for wtLiP and W171A, and the rates of decay were similar for both variants at each pH. These results indicate that the spontaneous decay of compound I may not be a result of the spontaneous electron transfer from amino acid Trp171 to the porphyrin π-cation radical, suggesting that electron transfer does not occur in the absence of VA. The binding of VA to wtLiP probably initiates the transfer of electrons from VA via Trp171 to the heme edge, resulting in oxidized VA. A possible through-protein electron-transfer pathway will need to be determined. The direct pathway from Trp171 to the proximal histidine ligand of the heme, His176, via the protein backbone is approximately 21.5 Å. An alternative 12.7-Å-long pathway runs partly through the protein backbone and includes two hydrogen bonds. Mutation studies on the amino acids between Trp171 and His176 may indicate a possible shortcut through the side chain of one of these residues to the heme.

The local environment near Trp171, the apparent site of VA oxidation, is acidic and highly conserved (Figure 6) (*23*). In addition to Trp171, the amino acids Asp165, Glu250, Lys260, and Phe267 are completely conserved among known LiP enzyme sequences, whereas Glu168 is only partly conserved. In LiPH8, Glu250, Asp264, and Lys260 appear to form an H-bonding network with the nitrogen of the Trp171 indole side chain, possibly orienting Trp171 in a fixed position (Figure 6). On the other side of Trp171, the acidic residues, Asp165 and Glu168, may be involved in the composition of the acidic environment, which has been proposed to stabilize $VA^{+\bullet}$ (*56*). However, at lower pH, these carboxylic residues, which have a typical pK_a of 4.4, are most

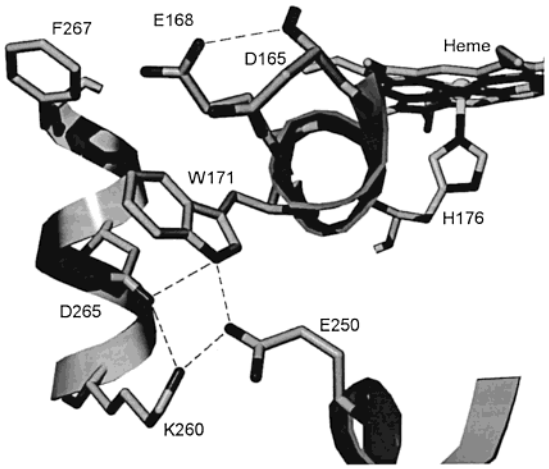

FIGURE 6: View of the protein environment surrounding Trp171 of LiP (*22*, *23*).

likely protonated, resulting in neutral side chains that are unable to stabilize the positively charged $VA^{+\bullet}$. Kinetic studies show that the activity for VA oxidation increases with decreasing pH from 6 to 3. Therefore, additional studies are required to elucidate the role of these acidic residues in LiP function.

The aromatic residue, Phe267, located near Trp171 (Figure 6) may be involved in the binding and oxidation of VA by a stacking interaction of the electron-rich π-systems of Trp171, VA, and Phe267. The aromatic character of this Trp171-centered VA binding site is disturbed by introduction of the F267L mutation. Kinetic analysis indicates that the steady-state oxidation of VA by F267L exhibited a ~3-fold increase in K_m. The transient-state kinetic analysis of F267L compound II reduction by VA exhibited a ~4-fold increase in K_D with no change in k_3 compared to wtLiP. Thus, both kinetic studies indicate that the F267L mutation affects VA binding to the enzyme, while the rate of oxidation remains similar to that of wtLiP.

In conclusion, these results indicate that mutations at the His82 and Gln222 positions in the heme access channel have little effect on VA oxidation, while a mutation at Trp171 eliminates the VA oxidation ability of the enzyme, confirming that Trp171 is essential for VA oxidation and suggesting that VA is oxidized at this site during catalysis. The local environment of Trp171 is involved in the binding of VA to this site as indicated by our results with the F267 mutation. The detailed mechanism of electron transfer from VA to the heme and the nature of the electron-transfer pathway await further studies.

NOTE ADDED AFTER ASAP POSTING

This article was inadvertently released ASAP on 02/02/02 before final corrections had been made. The correct version was posted 02/11/02.

REFERENCES

1. Gold, M. H., and Alic, M. (1993) *Microbiol. Rev. 57*, 605−622.
2. Welinder, K. G. (1992) *Curr. Opin. Struct. Biol. 2*, 388−393.
3. Buswell, J. A., and Odier, E. (1987) *CRC Crit. Rev. Biotechnol. 6*, 1−60.
4. Kirk, T. K., and Farrell, R. L. (1987) *Annu. Rev. Microbiol. 41*, 465−505.
5. Gold, M. H., Youngs, H. L., and Sollewijn Gelpke, M. D. (2000) in *Manganese and Its Role in Biological Processes* (Sigel, A., and Sigel, H., Eds.) Vol. 37, pp 559−586, Marcel Dekker, New York.
6. Renganathan, V., Miki, K., and Gold, M. H. (1986) *Arch. Biochem. Biophys. 246*, 155−161.
7. Schoemaker, H. E. (1990) *Recl. Trav. Chim. Pays-Bas 109*, 255−272.
8. Kersten, P. J., Tien, M., Kalyanaraman, B., and Kirk, T. K. (1985) *J. Biol. Chem. 260*, 2609−2612.
9. Joshi, D. K., and Gold, M. H. (1996) *Eur. J. Biochem. 237*, 45−57.
10. Hammel, K. E., Jensen, K. A., Jr., Mozuch, M. D., Landucci, L. L., Tien, M., and Pease, E. A. (1993) *J. Biol. Chem. 268*, 12274−12281.
11. Sheng, D., and Gold, M. H. (1998) *Biochemistry 37*, 2029−2036.
12. Sheng, D., and Gold, M. H. (1999) *Eur. J. Biochem. 259*, 626−634.
13. Hammel, K. E., Kalyanaraman, B., and Kirk, T. K. (1986) *J. Biol. Chem. 261*, 16948−16952.
14. Barr, D. P., and Aust, S. D. (1994) *Environ. Sci. Technol. 28*, 78A−87A.
15. Joshi, D. K., and Gold, M. H. (1994) *Biochemistry 33*, 10969−10976.
16. Tien, M., and Ma, D. (1997) *J. Biol. Chem. 272*, 8912−8917.
17. Leisola, M. S. A., Kozulic, B., Meussdoerffer, F., and Fiechter, A. (1987) *J. Biol. Chem. 262*, 419−424.
18. Andersson, L. A., Renganathan, V., Chiu, A. A., Loehr, T. M., and Gold, M. H. (1985) *J. Biol. Chem. 260*, 6080−6087.
19. Andersson, L. A., Renganathan, V., Loehr, T. M., and Gold, M. H. (1987) *Biochemistry 26*, 2258−2263.
20. de Ropp, J. S., La-Mar, G. N., Wariishi, H., and Gold, M. H. (1991) *J. Biol. Chem. 266*, 15001−15008.
21. Banci, L., Bertini, I., Kuan, I. C., Tien, M., Turano, P., and Vila, A. J. (1993) *Biochemistry 32*, 13483−13489.
22. Piontek, K., Glumoff, T., and Winterhalter, K. (1993) *FEBS Lett. 315*, 119−124.
23. Poulos, T. L., Edwards, S. L., Wariishi, H., and Gold, M. H. (1993) *J. Biol. Chem. 268*, 4429−4440.
24. Ritch, T. G., Jr., and Gold, M. H. (1992) *Gene 118*, 73−80.
25. Marquez, L., Wariishi, H., Dunford, H. B., and Gold, M. H. (1988) *J. Biol. Chem. 263*, 10549−10552.
26. Renganathan, V., and Gold, M. H. (1986) *Biochemistry 25*, 1626−1631.
27. Harvey, P. J., Palmer, J. M., Schoemaker, H. E., Dekker, H. L., and Wever, R. (1989) *Biochim. Biophys. Acta 994*, 59−63.
28. Dunford, H. B. (1999) *Heme Peroxidases*, Wiley-VCH, New York.
29. Wariishi, H., Huang, J., Dunford, H. B., and Gold, M. H. (1991) *J. Biol. Chem. 266*, 20694−20699.
30. Wariishi, H., Marquez, L., Dunford, H. B., and Gold, M. H. (1990) *J. Biol. Chem. 265*, 11137−11142.
31. Wariishi, H., and Gold, M. H. (1990) *J. Biol. Chem. 265*, 2070−2077.
32. Blodig, W., Doyle, W. A., Smith, A. T., Winterhalter, K., Choinowski, T., and Piontek, K. (1998) *Biochemistry 37*, 8832−8838.
33. Doyle, W. A., Blodig, W., Veitch, N. C., Piontek, K., and Smith, A. T. (1998) *Biochemistry 37*, 15097−15105.
34. Sollewijn Gelpke, M. D., Mayfield-Gambill, M., Cereghino, G. P. L., and Gold, M. H. (1999) *Appl. Environ. Microbiol. 65*, 1670−1674.
35. Alic, M., Letzring, C., and Gold, M. H. (1987) *Appl. Environ. Microbiol. 53*, 1464−1469.
36. Akileswaran, L., Alic, M., Clark, E. K., Hornick, J. L., and Gold, M. H. (1993) *Curr. Genet. 23*, 351−356.
37. Alic, M., and Gold, M. H. (1985) *Appl. Environ. Microbiol. 50*, 27−30.
38. Froeliger, E. H., Ullrich, R. C., and Novotny, C. P. (1989) *Gene 83*, 387−393.

39. Alic, M., Mayfield, M. B., Akileswaran, L., and Gold, M. H. (1991) *Curr. Genet. 19*, 491−494.
40. Mayfield, M. B., Kishi, K., Alic, M., and Gold, M. H. (1994) *Appl. Environ. Microbiol. 60*, 4303−4309.
41. Glenn, J. K., and Gold, M. H. (1985) *Arch. Biochem. Biophys. 242*, 329−341.
42. Gold, M. H., Kuwahara, M., Chiu, A. A., and Glenn, J. K. (1984) *Arch. Biochem. Biophys. 234*, 353−362.
43. Kulmacz, R. J. (1986) *Arch. Biochem. Biophys. 249*, 273−285.
44. Cheddar, G., Meyer, T. E., Cusanovich, M. A., Stout, C. D., and Tollin, G. (1989) *Biochemistry 28*, 6318−6322.
45. Gold, M. H., Wariishi, H., and Valli, K. (1989) *ACS Symp. Ser. No. 389*, 127−140.
46. Higuchi, T. (1990) *Wood Sci. Technol. 24*, 23−63.
47. Hatakka, A. (1994) *FEMS Microbiol. Rev. 13*, 125−135.
48. Harvey, P. J., Schoemaker, H. E., and Palmer, J. M. (1986) *FEBS Lett. 195*, 242−246.
49. Valli, K., Wariishi, H., and Gold, M. H. (1990) *Biochemistry 29*, 8535−8539.
50. Hammel, K. E., and Moen, M. A. (1991) *Enzyme Microb. Technol. 13*, 15−18.
51. Koduri, R. S., and Tien, M. (1995) *J. Biol. Chem. 270*, 22254−22258.
52. Koduri, R. S., and Tien, M. (1994) *Biochemistry 33*, 4225−4230.
53. Schoemaker, H. E., Lundell, T. K., Hatakka, A. I., and Piontek, K. (1994) *FEMS Microbiol. Rev. 13*, 321−332.
54. Smith, A. T., and Veitch, N. C. (1998) *Curr. Opin. Chem. Biol. 2*, 269−278.
55. Ambert-Balay, K., Fuchs, S. M., and Tien, M. (1998) *Biochem. Biophys. Res. Commun. 251*, 283−286.
56. Khindaria, A., Yamazaki, I., and Aust, S. D. (1996) *Biochemistry 35*, 6418−6424.

BI011930D